Dropwise Condensation Modeling Suitable for Superhydrophobic Surfaces

Sunwoo Kim
Assistant Professor
Department of Mechanical Engineering,
P.O. Box 755905,
University of Alaska,
Fairbanks, AK 99775
e-mail: swkim@alaska.edu

Kwang J. Kim
Professor
Department of Mechanical Engineering,
MS312,
Low Carbon Green Technology Laboratory
(LCGTL),
University of Nevada,
Reno, NV 89557
e-mail: kwangkim@unr.edu

A mathematical model is developed to represent and predict the dropwise condensation phenomenon on nonwetting surfaces having hydrophobic or superhydrophobic (contact angle greater than 150 deg) features. The model is established by synthesizing the heat transfer through a single droplet with the drop size distribution. The single droplet heat transfer is analyzed as a combination of the vapor-liquid interfacial resistance, the resistance due to the conduction through the drop itself, the resistance from the coating layer, and the resistance due to the curvature of the drop. A population balance model is adapted to develop a drop distribution function for the small drops that grow by direct condensation. Drop size distribution for large drops that grow mainly by coalescence is obtained from a well-known empirical equation. The evidence obtained suggests that both the single droplet heat transfer and drop distribution are significantly affected by the contact angle. More specifically, the model results indicate that a high drop-contact angle leads to enhancing condensation heat transfer. Intense hydrophobicity, which produces high contact angles, causes a reduction in the size of drops on the verge of falling due to gravity, thus allowing space for more small drops. The simulation results are compared with experimental data, which were previously reported. [DOI: 10.1115/1.4003742]

Keywords: dropwise condensation, contact angle, hydrophobicity, surface wettability, drop size distribution

1 Introduction

Since its discovery in 1930 by Schmidt et al. [1], dropwise condensation has attracted significant attention due to its superior heat transfer performance compared with filmwise condensation. It has been reported that dropwise condensation on a hydrophobic surface enhances heat transfer by an order of magnitude compared with filmwise condensation [2–5]. This stems from the fact that the absence of condensate film and the continuous surface renewal by falling large drops reduce the thermal resistance and improve the heat transfer. Unlike filmwise condensation where the liquid condensate forms a continuous film over the surface, dropwise condensation can be described as a combination of random processes such as initial drop formation, drop growth, and departure of large drops. In order to represent the phenomenon associated with this type of condensation, numerous researchers have attempted to establish mathematical models to be utilized for designing dropwise condensers.

One of the earliest dropwise condensation models was proposed by Le Fevre and Rose [6], who combined a calculation for the heat transfer through a single drop with a calculation for the drop size distribution. Their single drop heat transfer model considered the conduction resistance, the vapor-liquid interfacial matter transfer, the promoter layer resistance, and the resistance due to the convex liquid surface. For the drop size distribution, they used the concept of the surface area fraction occupied by drops equal to or larger than the drop size of interest. Based on this model, advanced models have followed by including more precise expressions for the growth of small drops. Tanaka [7] employed a population balance theory to evaluate the transient change of local drop size distribution by taking into account the two mechanisms of small drop's growth: direct condensation onto the drop and coalescence with neighboring drops. This enabled a more accurate prediction of drop size distribution for small drops, which was previously difficult to experimentally examine. The advancement made from Tanaka's model was remarkable in that it is true that most of the heat transfer takes place through small drops [8,9]. Since that time, the population balance theory has been used to estimate the population of drops of a given size. Wu and Maa [8] derived the drop size distribution of small drops under the assumption of a steady size distribution using the population balance concept. Maa [10] later utilized the concept to solve the drop size distribution for both small and large drops. Abu-Orabi [11] refined the previous dropwise condensation models based on population balance theory by considering all possible thermal resistances.

Despite the amount of research effort on dropwise condensation modeling, none of the previous models adequately represents this type of condensation occurring on a surface whose hydrophobic feature leads to a contact angle greater than 90 deg. They assumed that the shape of drops is fixed to be hemispherical, i.e., the contact angle is held constant at 90 deg. This assumption makes the previous models improper for enhanced hydrophobic surfaces, which generate a water-contact angle greater than 90 deg. For example, it has been reported that organic self-assembled monolayer (SAM) coatings possibly create contact angles ranging from 110 deg to 150 deg [12–14]. Also, it should be noted that modern nanotechnology has encouraged scientists in the field of dropwise condensation to develop a condensing surface with strong hydrophobicity because it is believed that such surfaces promote the drop movement and departure and consequently accelerate surface renewal, allowing small drops to form.

The objective of the current study is to develop a mathematical model for the calculation of dropwise condensation heat transfer for superhydrophobic surface treatments. Unlike previous models, the current model is capable of incorporating contact angles greater than 90 deg. Both the heat transfer through a single drop with a given size and the drop size distribution are modeled while the contact angle of the drop with the condensing surface is con-

Contributed by the Heat Transfer Division of ASME for publication in the JOURNAL OF HEAT TRANSFER. Manuscript received December 25, 2009; final manuscript received February 25, 2011; published online May 3, 2011. Assoc. Editor: S. A. Sherif.

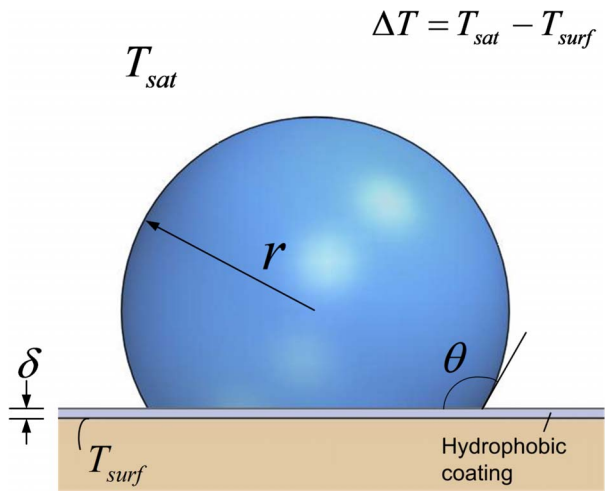

Fig. 1 A droplet on the condensing surface coated with hydrophobic material

sidered as a variable. The contact angle highly affects the thermal resistances corresponding to the conduction through the drop and the vapor-to-liquid interfacial heat transfer since the resistances are dependent on the shape, interfacial surface area, and volume of the drop. Drop size distributions are calculated via the previously employed population balance theory for the initial stages of drop formation and drop growth by direct condensation while the well established distribution model proposed by Le Fevre and Rose [6] is adopted for the larger drop sizes. The present model computes the overall heat transfer rate by dropwise condensation and evaluates the effect of the contact angle on the heat transfer performance. In addition, the effect of the promoter (coating) layer is also addressed in terms of the promoter thickness and the number of nucleation sites on it.

2 Single Drop Heat Transfer Model

During dropwise condensation, drops form and grow on the condensing surface, and then depart from the condensing surface. Each drop contributes to the condensation process by transferring heat through itself. Therefore, determining the amount of heat transferred through a single drop is necessary in predicting the overall heat transfer by dropwise condensation.

The first step toward developing a model of heat transfer through a single drop is to recognize all contributing thermal resistances between the saturation temperature of the vapor and the temperature of the condensing surfaces. For the present model, the thermal resistances are composed of the vapor-liquid interfacial resistance, the resistance due to the conduction through the drop itself, the resistance from the coating layer, and the resistance due to the curvature of the drop. It should be noted that the present model does not take into account the effect of convection happening inside the droplet. The convection was neglected in this paper by assuming that drops are sufficiently small such that conduction is the primary mechanism of heat transfer through the droplet.

Consider a drop with radius r on a plain surface that is coated with a hydrophobic material, as shown in Fig. 1. The contact angle θ on the coated surface is assumed to be fixed regardless of the drop size r and the vapor and surface temperatures. Knowing the vapor saturation temperature T_{sat} and the plate surface temperature T_{surf}, the heat transfer rate q can be derived by considering all resistances.

For the purposes of this model, all resistances will be presented as the temperature drop for the region in question. The vapor-liquid interfacial resistance is responsible for the temperature drop ΔT_i between the vapor and the drop surface. It is represented as

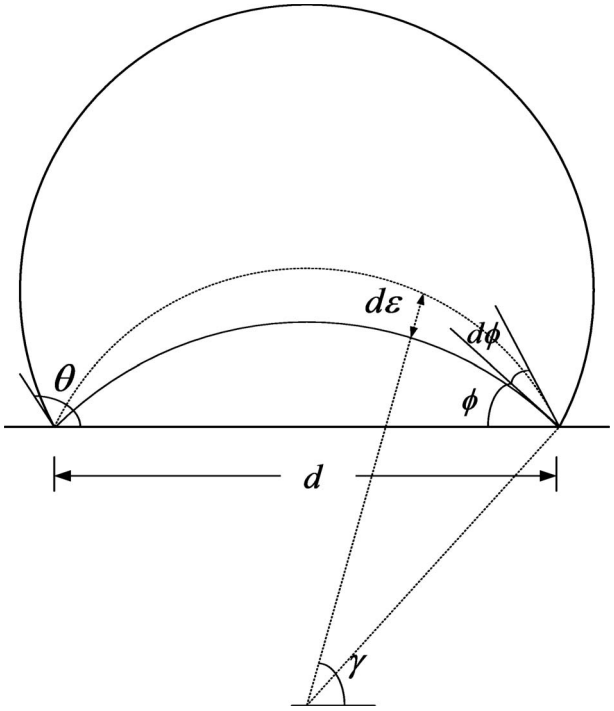

Fig. 2 Heat transfer by conduction between two neighboring isothermal surfaces

$$\Delta T_i = \frac{q_d}{h_i 2\pi r^2 (1 - \cos\,\theta)} \tag{1}$$

where q_d is the heat transfer rate through the droplet and h_i is the interfacial heat transfer coefficient, which strongly depends on the vapor pressure. Tanasawa [15] reported that for water vapor dropwise condensation, h_i varies from 0.383 $\text{MW/m}^2\,\text{K}$ to 15.7 $\text{MW/m}^2\,\text{K}$ for a pressure ranging from 0.01 atm to 1.0 atm, respectively.

The droplet itself acts as the resistance to heat conduction through the droplet. In order to analyze heat conduction, a method of integration of the temperature difference between two neighboring isothermal surfaces is introduced. The heat is thought to conduct from one isothermal surface having an angle of ϕ (see Fig. 2) to another isothermal surface of angle $\phi+d\phi$. The surface area of the lower isothermal surface A_s is obtained by integration with respect to the angle γ,

$$dA_s = 2\pi\left(\frac{d}{2}\frac{1}{\sin\,\phi}\right)^2 \cos\,\gamma d\gamma \tag{2}$$

$$A_s = \int_{(\pi/2)-\phi}^{(\pi/2)} \frac{\pi d^2}{2\,\sin^2\,\phi}\cos\,\gamma d\gamma \tag{3}$$

$$A_s = \frac{\pi d^2}{2}\frac{1 - \cos\,\phi}{\sin^2\,\phi} \tag{4}$$

The distance $d\varepsilon$ between the two isothermal surfaces is the largest at $\gamma=90$ deg,

$$d\varepsilon_{\max} = \frac{d}{2}((\csc(\phi+\Delta\phi) - \csc\ \phi) - (\cot(\phi+\Delta\phi) - \cot\ \phi))$$

$$= \frac{d}{2}(\csc'\phi d\phi - \cot'\phi d\phi) = \frac{d}{2}(\csc^2\phi - \cot\ \phi\ \csc\ \phi)d\phi \tag{5}$$

The mean distance is assumed to be half of the maximum distance $d\varepsilon_{\max}$,

$$d\bar{\varepsilon} = \frac{d}{4}(\csc^2\ \phi - \cot\ \phi\ \csc\ \phi)d\phi \tag{6}$$

The temperature difference ΔT_{drop} between the drop surface and the coating surface is calculated by integration with respect to the angle ϕ,

$$\Delta T_{\text{drop}} = \int_0^\theta \frac{q_d}{k_c}\frac{d\bar{\varepsilon}}{A_s} = \frac{q_d}{k_c}\frac{d}{4}\frac{2}{\pi d^2}\int_0^\theta \frac{(\csc^2\ \phi - \cot\ \phi\ \csc\ \phi)\sin^2\ \phi}{1-\cos\ \phi}d\phi$$

$$= \frac{q_d}{k_c}\frac{1}{2\pi d}\int_0^\theta d\phi \tag{7}$$

The temperature drop caused by conduction through the drop can now be written as

$$\Delta T_{\text{drop}} = \frac{q_d\theta}{2k_c\pi d} \tag{8}$$

where $d=2r\ \sin\ \theta$. This allows Eq. (8) to be rewritten as

$$\Delta T_{\text{drop}} = \frac{q_d\theta}{4\pi r k_c\ \sin\ \theta} \tag{9}$$

Most previous models assuming that the droplet is hemispherical employed Fatica and Katz's [16] modeling work to obtain ΔT_{drop} when $\theta=90$ deg, whereas the result from Eq. (9) does not exactly agree with their temperature difference analysis. This disagreement is because Fatica and Katz discretized the volume of the droplet using isothermal and equiflux surfaces before numerically calculating the average heat transfer coefficient on the surface in contact with the solid by integrating the thermal resistances of the volume elements. In contrast, the fully analytical result of Eq. (9) suggests that the temperature difference through hemispherical droplets is approximately 1.5 times greater than Fatica's analysis.

The temperature drop due to the resistance of the coating material on the contact surface is given by

$$\Delta T_{\text{coat}} = \frac{q_d\delta}{k_{\text{coat}}\pi r^2\ \sin^2\ \theta} \tag{10}$$

In Eq. (10), the impact of phonon dispersion on the thermal conductivity k_{coat} is assumed to be negligible.

From the literature [6], the temperature drop ΔT_c due to the drop curvature is found to be

$$\Delta T_c = \frac{2T_{\text{sat}}\sigma}{H_{fg}r\rho} \tag{11}$$

Since the wall subcooling determines the minimum viable drop radius [17],

$$r_{\min} = \frac{2T_{\text{sat}}\sigma}{H_{fg}\rho\Delta T} \tag{12}$$

Equation (11) is reduced to

$$\Delta T_c = \frac{r_{\min}}{r}\Delta T \tag{13}$$

The total temperature difference between the vapor and the plate surface is the sum of the four temperature drops found in Eqs. (1)–(13),

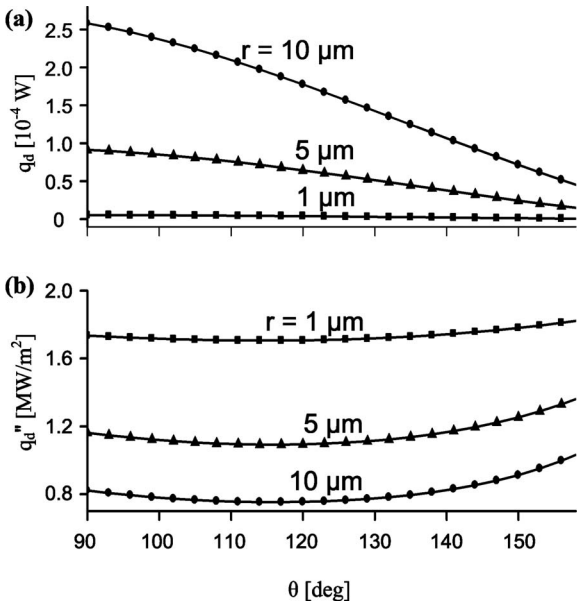

Fig. 3 Single drop heat transfer rate and heat flux with respect to the contact angle

$$\Delta T = \Delta T_i + \Delta T_{\text{drop}} + \Delta T_{\text{coat}} + \Delta T_c = q_d\frac{1}{\pi r^2}\frac{1}{1-r_{\min}/r}\left(\frac{\delta}{k_{\text{coat}}\sin^2\ \theta} + \frac{r\theta}{4k_c\ \sin\ \theta} + \frac{1}{2h_i(1-\cos\ \theta)}\right) \tag{14}$$

Therefore, the heat transfer rate through a drop of radius r is expressed as

$$q_d = \frac{\Delta T\pi r^2(1-r_{\min}/r)}{\left(\frac{\delta}{k_{\text{coat}}\sin^2\ \theta} + \frac{r\theta}{4k_c\ \sin\ \theta} + \frac{1}{2h_i(1-\cos\ \theta)}\right)} \tag{15}$$

Equation (15) demonstrates that the heat transfer rate q_d varies with the drop size, the contact angle, and the thickness of the coating layer.

The equation provides an estimated heat transfer rate, as shown in Fig. 3(*a*). Here, the vapor saturation temperature of 373 K, a vapor to solid surface temperature difference of 10 K, and a 1 μm thick coating with a thermal conductivity of 0.2 W/m K were assumed. For the condition that condensate develops dropwise ($\theta>90$ deg), the heat transfer rate for a drop having a fixed radius decreases as its contact angle increases. This is explained by the fact that even though a higher contact angle induces a larger liquid-vapor interface (the third term in the denominator in Eq. (15)), it raises the total resistance to conduction induced by drop volume (the second term in the denominator in Eq. (15)) and reduces the contact area between the drop and the coating surface. Hence, a smaller drop ($r=1$ μm) transfers less heat than a larger drop ($r=5,10$ μm) because it has less liquid-solid contact area.

However, a larger heat flux on the liquid-solid contact is estimated for a smaller drop as Fig. 3(*b*) indicates. This means that a condensation surface covered by small drops provides a better condensation performance than the same surface covered by large drops. This is consistent with the results found in previous studies [8,9], which report that more condensation heat transfer occurs through small drops. Thus, the performance of dropwise condensation highly depends on the rate of sweeping, which makes nucleation sites available to newly forming drops. In addition to the sweeping rate, the size and population of maximum drops have a significant impact on dropwise condensation in that the area occupied by large drops is considered to be an ineffective

heat transfer surface. Figure 3(*b*) also shows how the contact angle affects the heat flux. For a fixed size drop, the heat flux can be increased by having a contact angle higher than the critical value (approximately 110–120 deg), implying that a superhydrophobic surface with a contact angle of 150 deg or more may produce a superior heat transfer during dropwise condensation.

3 Drop Size Distribution

Drop nucleation occurs at proper nucleation sites with the initial drop growing primarily by direct deposition from the vapor onto the drop surface. As the drops become larger and as the distances between neighboring droplets become smaller, coalescence begins to be the dominating mechanism for drop growth until it departs and falls off. When the drop grows to the departure size, the sum of gravity and other external forces exceeds the capillary force and causes it to fall and sweep away all drops in its path. The falling drop clears the condensing surface so that new initial droplets can be formed. As a result of this growth from the nucleation through the departure, there are droplets of many sizes on the condensing surface [18].

For small drops that grow mainly by direct condensation, the population balance theory [7–11] can be employed to determine drop size distribution. The derivation of the steady state drop size distribution is based on the conservation of the number of drops in a certain size range, i.e., the number of drops entering a size range must equal the number of drops leaving the same size range. This analysis assumes that the contact angle remains the same from the drop nucleation through the departure from the surface, i.e., there exists only one contact angle for all the drops of different sizes on the surface.

We consider the population balance for an arbitrary size range r_1-r_2. The drop growth rate is defined as [11,17]

$$G = \frac{dr}{dt} \tag{16}$$

The growth rates of drops of radii r_1 and r_2 are called G_1 and G_2, respectively. The population density of drops $n(r)$ is defined as the number of drops of radius r per unit area. For example, n_1 denotes the population density of drops of radius r_1, and n_2 the population density of drops of radius r_2. The number of drops that enter this range for a differential increment of time dt can be expressed as An_1G_1dt, where A is the area of an arbitrary section of the condensing surface. In a similar fashion, the number of drops leaving by growth is An_2G_2dt. Drops in this size range are also removed by the sweeping flow of large falling drops. The number of drops swept off is $Sn_{1-2}\Delta rdt$, where S is the sweeping rate at which the substrate surface is renewed by falling drops, n_{1-2} is the average population density in the size range r_1 and r_2, and Δr equals r_2-r_1. In order for the number of drops to be conserved in this size range, the number of drops entering by growth must equal the sum of the number of drops leaving by growth and the number of drops swept away by larger drops, i.e.,

$$An_1G_1dt = An_2G_2dt + Sn_{1-2}\Delta rdt \tag{17}$$

Equation (17) can be simplified as

$$A(G_2n_2 - G_1n_1) = -Sn_{1-2}\Delta r \tag{18}$$

As Δr approaches zero, n_{1-2} becomes a point value, and the equation can now be written as

$$\frac{d}{dr}(Gn) + \frac{n}{\tau} = 0 \tag{19}$$

where the sweeping period $\tau = A/S$.

The heat transfer rate through a drop of radius r equals to the rate at which the enthalpy of newly condensing vapor changes, and therefore one can write the single drop heat transfer q_d as a function of the drop growth rate G:

$$q_d = \rho H_{fg} 2\pi r^2 (1-\cos\theta) G \tag{20}$$

Substituting Eq. (20) into Eq. (15) produces the drop growth rate as a function of the radius r:

$$G = \frac{\Delta T}{2\rho H_{fg}} \frac{1 - r_{\min}/r}{\dfrac{r\theta(1-\cos\theta)}{4k_c \sin\theta} + \dfrac{\delta(1-\cos\theta)}{k_{\text{coat}} \sin^2\theta} + \dfrac{1}{2h_i}} = A_1 \frac{1 - r_{\min}/r}{A_2 r + A_3} \tag{21}$$

where

$$A_1 = \frac{\Delta T}{2\rho H_{fg}} \tag{22}$$

$$A_2 = \frac{\theta(1-\cos\theta)}{4k_c \sin\theta} \tag{23}$$

$$A_3 = \frac{1}{2h_i} + \frac{\delta(1-\cos\theta)}{k_{\text{coat}} \sin^2\theta} \tag{24}$$

Because G is a function of r, Eq. (19) can be integrated with respect to r,

$$\int_{(Gn)_{\min}}^{Gn} \frac{d(Gn)}{Gn} = \int_{r_{\min}}^{r} \frac{-dr}{G\tau} \tag{25}$$

By solving Eq. (25), we obtain

$$n(r) = \frac{(Gn)_{\min}}{G} \exp\left(\frac{A_2}{\tau A_1} \left[\frac{(r - r_{\min}^2)}{2} + 2r_{\min}(r - r_{\min}) + r_{\min}^2 \ln(r - r_{\min}) \right] + \frac{A_3}{\tau A_1} [r - r_{\min} + r_{\min} \ln(r - r_{\min})] \right) \tag{26}$$

Now, Eq. (26) provides the drop size distribution for small drops, which grow mainly by direct condensation.

For large drops, the drop size distribution $N(r)$ was established by Le Fevre and Rose [6],

$$N(r) = \frac{1}{3\pi r^2 r_{\max}} \left(\frac{r}{r_{\max}} \right)^{-2/3} \tag{27}$$

The effective maximum drop radius (the size of departure drops) $r_{\max}$ can be estimated based on the force balance between surface tension and gravity. When the drop-surface contact area is close to a circle, the capillary force can be simplified as [19,20]

$$F_c \approx cd\sigma(\cos\theta_r - \cos\theta_a) = c2r \sin\theta\sigma(\cos\theta_r - \cos\theta_a) \tag{28}$$

where θ_r and θ_a refer to the receding contact angle and the advancing contact angle, respectively, and c is a numerical constant that depends on the shape of the drop and on the steepness of the substrate surface. Furthermore, the gravity on the drop is

$$F_g = \frac{2 - 3\cos\theta + \cos^3\theta}{3} \pi r^3 \rho g \tag{29}$$

From the force balance between Eqs. (28) and (29), the radius of departure drops can be deduced:

$$r_{\max} = \left(\frac{6c(\cos\theta_r - \cos\theta_a)\sin\theta}{\pi(2 - 3\cos\theta + \cos^3\theta)} \frac{\sigma}{\rho g} \right)^{1/2} \tag{30}$$

When the effective radius r_e is defined as the boundary between the small drops $n(r)$ and large drops $N(r)$ and the nucleation sites are assumed to form a square array, we can write

$$r_e = (4N_s)^{-1/2} \tag{31}$$

where N_s is the number of nucleation sites on a unit area of condensing surface. Because the population density ($n(r)$ and $N(r)$) with respect to the drop size r should satisfy continuity at the

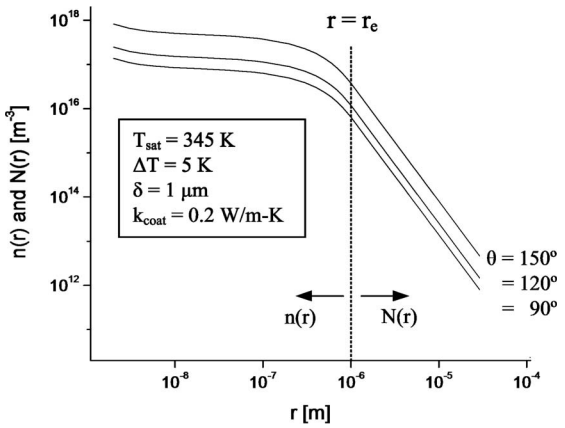

Fig. 4 Drop size distributions for contact angles of 90 deg, 120 deg, and 150 deg

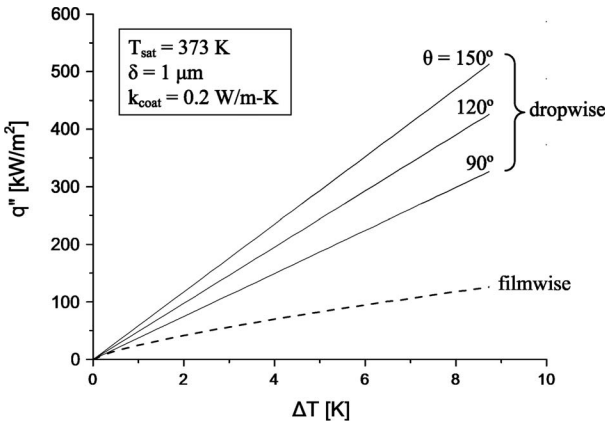

Fig. 5 Overall heat transfer rate per unit area versus vapor to solid surface temperature difference for contact angles of 90 deg, 120 deg, and 150 deg in comparison with filmwise condensation

boundary, a boundary condition is set as $n(r)=N(r)$ at $r=r_e$. This solves $(Gn)_{\min}$, one of the unknowns in Eq. (26), resulting in

$$n(r)=\frac{1}{3\pi r_e^3 r_{\max}}\left(\frac{r_e}{r_{\max}}\right)^{-2/3}\frac{r(r_e-r_{\min})}{r-r_{\min}}\frac{A_2 r+A_3}{A_2 r_e+A_3}\exp(B_1+B_2) \tag{32}$$

where

$$B_1=\frac{A_2}{\tau A_1}\left[\frac{r_e^2-r^2}{2}+r_{\min}(r_e-r)-r_{\min}^2\ln\left(\frac{r-r_{\min}}{r_e-r_{\min}}\right)\right] \tag{33}$$

$$B_2=\frac{A_3}{\tau A_1}\left[r_e-r-r_{\min}\ln\left(\frac{r-r_{\min}}{r_e-r_{\min}}\right)\right] \tag{34}$$

The other unknown, the sweeping period τ, can also be expressed as a function of r_e by taking the second boundary condition $d(\ln n(r))/d(\ln r)=d(\ln N(r))/d(\ln r)=-8/3$,

$$\tau=\frac{3r_e^2(A_2 r_e+A_3)^2}{A_1(11A_2 r_e^2-14A_2 r_e r_{\min}+8A_3 r_e-11A_3 r_{\min})} \tag{35}$$

The drop size distribution obtained from Eqs. (27) and (32) is presented in Fig. 4. Three curves were plotted for the contact angles of 90 deg, 120 deg, and 150 deg under assumptions that the vapor temperature is 345 K and the number of nucleation sites is 2.5×10^{11} m^{-2}, and the other conditions presented in the graph (Fig. 4). The curves in the left side region of the dashed line ($r=r_e$) represent the population density for small drops $n(r)$ and those in the right side region of the dashed line show the population density for large drops $N(r)$. The plot indicates that on a certain area of condensing surface, there are numerous small drops and relatively few large drops. In other words, the population density decreases with an increase in drop size. Sweeping and coalescence explain this phenomenon. For small drops, not all of the smallest drops grow to the effective radius r_e because some are swept off by departure drops. For large drops, drop growth primarily occurs when two or more drops coalesce into one; however, sweeping still affects the population density in the same fashion as it does for small drops. The declining slope of the population density for large drops is steeper than for small drops because large drops experience coalescence in addition to being swept.

Another significant finding from Fig. 4 is that a higher contact angle leads to a larger density for a certain drop size, showing a shift-up in the graph. However, the contact angle does not significantly affect the shape of the curves; rather change in the contact angle leads to change in the effective maximum drop radius (Eq. (30)). When a drop has a large contact angle, $r_{\max}$ becomes smaller (the first fraction in the right side in Eq. (30) is reduced as θ increases). It is evident that as the contact angle becomes high, the attractive force between the drop and the solid surface becomes weak while the increase in the total volume yields increasing gravitational force. Consequently, drop departure happens at a smaller drop size. Reducing the effective maximum drop radius means more surface area for small drops, clearly seen in Fig. 4 as the increase of drop population density with increased contact angle.

4 Dropwise Condensation Heat Transfer Rate

The steady state dropwise condensation heat transfer rate per unit area of the condensing surface can be obtained by multiplying the heat transfer rate through a single drop with the population density,

$$q''=\int_{r_{\min}}^{r_e} q_d(r)n(r)dr+\int_{r_e}^{r_{ram}} q_d(r)N(r)dr \tag{36}$$

The present model utilizing the results of Eq. (36) predicts the heat transfer rate per unit area for the contact angles of 90 deg, 120 deg, and 150 deg in Fig. 5. For the calculation, the following conditions were used: The vapor saturation temperature was 373 K, the nucleation density was 2.5×10^{11} m^{-2}, and the thermal conductivity and thickness of the coating layer were 0.2 W/m K and 1 μm, respectively. A curve for the Nusselt analysis is also presented for a comparison with filmwise condensation under the same conditions with the exception of the absence of the coating layer. The comparison to filmwise condensation reveals that the dropwise condensation is a superior mechanism to the filmwise condensation despite the additional thermal barrier from the coating for the dropwise method. The smallest heat flux among the dropwise condensation cases, which comes from the contact angle of 90 deg, is 213% greater than the heat flux from the filmwise for the subcooling of 4 K. The enhancement from the filmwise to the dropwise condensation of 90 deg contact angle becomes even larger for a large subcooling ΔT. When ΔT is 8 K, the ratio of 90 deg contact angle dropwise to filmwise heat flux is calculated as 2.53 (and 2.13 when $\Delta T=4$ K). This is attributed to the waning slope of heat flux q'' along the abscissa while the heat fluxes of dropwise condensation are nearly proportional to the subcooling. For filmwise condensation, as a larger subcooling drives a greater mass flow of condensate, the condensate film on the surface becomes thicker, and hence the thermal resistance increases with the subcooling. In contrast, the subcooling does not nearly affect the drop size distribution for dropwise condensation because the size

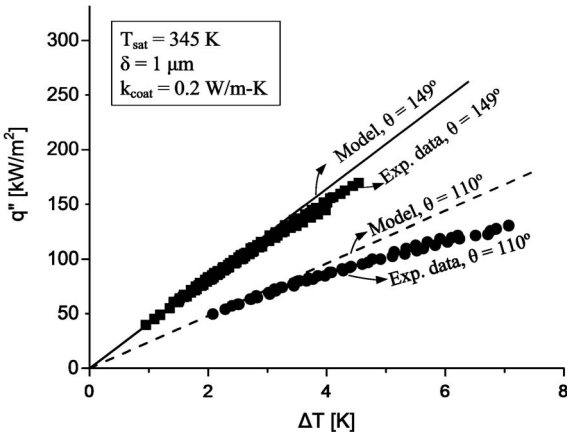

Fig. 6 Model prediction and experimental results for overall heat transfer rate per unit area at a condenser pressure of 33.86 kPa

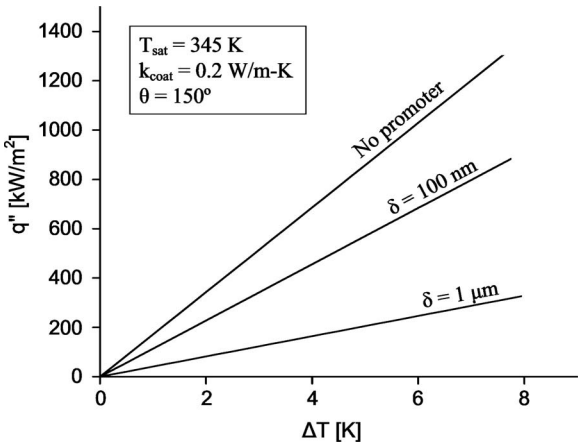

Fig. 7 Overall heat flux versus vapor subcooling for different thicknesses of coating layer

of the maximum droplets (departure drops) remains constant. A high subcooling, however, increases the drop growth rate G and decreases the sweeping period τ.

The effect of the contact angle on the heat transfer by dropwise condensation appears remarkable: A high contact angle produces a large heat transfer rate. The condensation heat transfer coefficient ($q''/\Delta T$) for the contact angle of 90 deg is nearly constant at 37.3 kW/m^2 K, which can be improved to 48.7 kW/m^2 K and 58.6 kW/m^2 K by promoting the contact angles to 120 deg and 150 deg, respectively. These are improvements of 30% and 57%, respectively. As discussed in the previous section, a high contact angle leads to lowering the effective maximum drop radius, resulting in more small drops. Moreover, more heat is transferred through small drops than large drops [8,9]. This can also be proved by the analysis for single drop heat transfer. In Fig. 3, a smaller drop appears to create more heat flux on the contact surface. Thus, in conclusion, a better heat transfer performance by dropwise condensation is obtained with a high contact angle.

The present model is compared with the results of the experimental study reported by Vemuri and Kim [13] and Vemuri et al. [14] in Fig. 6. Their group investigated the performance of heat transfer by dropwise condensation promoted by a SAM coating technique. They attempted a difference method for processing the coating materials and fabricated two SAM layers, which generate water-contact angles of 110 deg and 149 deg. The overall heat transfer rate was measured for a horizontal round tube at the condenser pressure of 33.86 kPa. Figure 6 shows that the model properly predicts the condensation heat transfer. Both the model and the experiments exhibit the difference in heat flux between hydrophobic (110 deg) and nearly superhydrophobic (149 deg) surfaces. The experimental data, however, show a decreased inclination of the heat flux versus the subcooling, unlike the prediction made by the model. At a subcooling of 6 K, the simulation predicts a 17.8% greater heat flux than the experimental data for the case of θ=110 deg. A similar divergence was observed from the comparison of θ=149 deg with a moderate error of 8.6% at a subcooling of 4 K. Nevertheless, it should be emphasized that the data and model are in excellent agreement in a low subcooling region where more reliable data are collected. At a high subcooling, the life cycle of dropwise condensation likely breaks and becomes partially filmwise due to an excessive mass flow rate of the condensate. If dropwise condensation happens on the entire condensing surface, the heat transfer should be proportional to the subcooling as the heat transfer through a drop increases linearly with the temperature difference while the drop distribution is hardly affected by the temperature difference. Therefore, one can conclude from Fig. 6 that the present model successfully describes dropwise condensation heat transfer by taking into account the effect of the contact angle.

5 The Coating Layer

Dropwise condensation of water on metal surfaces is hardly observed in natural conditions and thus is generally promoted with a proper coating layer. An understanding of the coating layer (promoter) is critical not only because it determines the surface wettability but because it adds an extra thermal resistance. The nucleation density is also dependent on the layer surface. The model is here utilized for quantifying the effect of the coating layer and for designing an effective promoter.

It is obvious that a thin layer is preferred because the thermal resistance is minimal. Figure 7 displays a model prediction of overall heat flux for coating layers of different thicknesses. The computation was carried out when the layer with the thermal conductivity of 0.2 W/m K creates a 150 deg contact angle at the condenser pressure of 33.86 kPa. The overall heat flux is significantly influenced by the thickness. When the 1 μm thick promoter reduces its thickness to 100 nm without any change in the contact angle or the nucleation density, the heat transfer performance will improve by a factor of 2.8. If the same hydrophobicity can be achieved without any promoter (on a bare surface), the condensing surface can produce 1.5 times the heat transfer of the 100 nm thick promoter and 4.2 times that of the 1 μm promoter, respectively. This result implies that a redundantly thick coating results in a significant degradation in heat transfer.

A parameter study on the number of nucleation sites is also presented for the promoter surfaces having the nucleation densities N_s of 1×10^{10} m^{-2}, 1×10^{11} m^{-2}, and 1×10^{12} m^{-2} in Fig. 8. The nucleation density exhibits a clear correlation to the overall heat flux. A high density of nucleation sites creates large overall heat flux on the condensing surface. The coating surface with 1×10^{12} m^{-2} rejects 23% more heat over the 1×10^{11} m^{-2} surface and 61% more over the 1×10^{10} m^{-2} surface throughout the subcooling range shown in Fig. 8. From the viewpoint of the current model, a high density of nucleation sites leads to a decrease in the size of drops, which experience their first coalescence (r_e). This early coalescence allows spaces for new initial drops, causing a high population of small drops. One can conclude that a well-structured superhydrophobic surface providing more nucleation sites is desirable for dropwise condensation.

6 Conclusion

Although the concepts of dropwise condensation were introduced more than four decades ago, there has been no model into

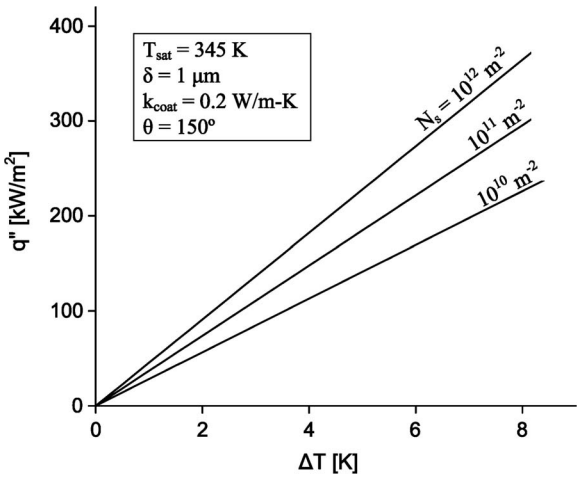

Fig. 8 Overall heat flux versus subcooling for different nucleation densities

which the effect of contact angle has been incorporated. For the same period, numerous researchers accomplished effective and sophisticated hydrophobic coatings. Thus, understanding the effect of contact angle on dropwise condensation has become more important. This research may be an answer for the current demand in the field of dropwise condensation.

A single drop heat transfer model taking account for the effect of contact angle was developed. The model considered all the thermal resistances between the vapor and the condenser surface. It was shown that a smaller drop can transfer more heat per contact area (higher heat flux), and the heat flux can be increased even more with high contact angles. In addition, the single drop heat transfer model led to a drop size distribution that is dependent on the contact angle. This showed that the contact angle is a critical parameter for determining the effective maximum drop radius (the size of departure drops). High contact angles reduce the size of departure drops, allowing more condensing surface for small drops. Finally, the overall dropwise condensation heat transfer rate was calculated by multiplying the heat transfer rate through a single drop with the population density. Condensation with high contact angles achieved a better performance.

In addition, the impacts of the thickness and structure of the coating layer were analyzed and it was seen that thick coating negates the improvement from superhydrophobic surfaces because of its poor thermal conductance. Consequently, a rough surface could be preferable for the coating structure since it can create more nucleation sites, producing increased nucleation density.

Acknowledgment

The authors acknowledge the financial support from the National Renewable Energy Laboratory (NREL) (Grant Nos. NDJ-7-77250-1 and NAX-9-66014-05). Also, special thanks go to Lynn Billman and Dr. Keith Gawlik of NREL.

Nomenclature

A = area of the condensing surface, m^2
A_s = area of an arbitrary isothermal surface, m^2
c = constant dependent on the geometry of drop and surface, Eq. (28)
d = contact diameter of droplet, m
dt = distance between two arbitrary isothermal surfaces, m
F_c = capillary force, N
F_g = gravity on drop, N
g = gravitational acceleration, m/s^2
G = drop growth rate, m/s
h_i = interfacial heat transfer coefficient, W/m^2 K
H_{fg} = latent heat of vaporization, J/kg
k_c = thermal conductivity of the condensate, W/m K
k_{coat} = thermal conductivity of the coating material, W/m K
n = population density of small drops, m^{-3}
N = population density of large drops, m^{-3}
N_s = number of nucleation site per unit area of condensing surface, m^{-2}
q = heat transfer rate, W
q_d = heat transfer rate through droplet, W
q'' = heat flux, W/m^2
r = drop radius, m
r_e = effective drop radius, m
r_{max} = effective maximum drop radius, m
r_{min} = minimum drop radius, m
S = surface renewal rate due to sweeping of large falling drops, m^2/s
t = time, s
T_{sat} = vapor saturation temperature, K
T_{surf} = condensing surface temperature, K

Greek Letters

γ = angle in Fig. 2
δ = thickness of the coating layer, m
ε = distance between isothermal surfaces in Fig. 2, m
ΔT = surface subcooling temperature, K
ΔT_c = temperature drop due to drop curvature, K
ΔT_{coat} = temperature drop due to conduction through coating layer, K
ΔT_{drop} = temperature drop due to conduction through drop, K
ΔT_i = temperature drop due to interfacial resistance, K
θ = contact angle
θ_a = advancing contact angle
θ_r = receding contact angle
ρ = density of the condensate, kg/m^3
σ = surface tension, N/m
τ = sweeping period, s
ϕ = angle in Fig. 2

References

[1] Schmidt, E., Schurig, W., and Sellschopp, W., 1930, "Versuche über die Kondensation von Wasserdampf in Film- und Tropfenform," Forsch. Ingenieurwes., **1**(2), pp. 53–63.
[2] Welch, J., and Westwater, J. W., 1961, "Microscopic Study of Dropwise Condensation," ASME International Developments in Heat Transfer, **2**, pp. 302–309.
[3] Le Fevre, E. J., and Rose, J. W., 1964, "Heat-Transfer Measurements During Dropwise Condensation of Steam," Int. J. Heat Mass Transfer, **7**, pp. 272–273.
[4] Kandlikar, S. G., Shoji, M., and Dhir, V. K., 1999, *Handbook of Phase Change: Boiling and Condensation*, Taylor & Francis, Philadelphia, PA.
[5] Ma, X., Rose, J. W., Xu, D., Lin, J., and Wang, B., 2000, "Advances in Dropwise Condensation Heat Transfer: Chinese Research," Chem. Eng. J., **78**(2–3), pp. 87–93.
[6] Le Fevre, E. J., and Rose, J. W., 1966, "A Theory of Heat Transfer by Dropwise Condensation," Proceedings of the Third International Heat Transfer Conference, Chicago, IL, Vol. 2, pp. 362–375.
[7] Tanaka, H., 1975, "A Theoretical Study of Dropwise Condensation," ASME J. Heat Transfer, **97**, pp. 72–98.
[8] Wu, W. H., and Maa, J. R., 1976, "On the Heat Transfer in Dropwise Condensation," Chem. Eng. J., **12**(3), pp. 225–231.
[9] Neumann, A. W., Abdelmessih, A. H., and Hameed, A., 1978, "The Role of Contact Angles and Contact Angle Hysteresis in Dropwise Condensation Heat Transfer," Int. J. Heat Mass Transfer, **21**(7), pp. 947–953.
[10] Maa, J. R., 1978, "Drop Size Distribution and Heat Flux of Dropwise Condensation," Chem. Eng. J., **16**(3), pp. 171–176.
[11] Abu-Orabi, M., 1998, "Modeling of Heat Transfer in Dropwise Condensation," Int. J. Heat Mass Transfer, **41**(1), pp. 81–87.
[12] Das, A. K., Kilty, H. P., Marto, P. J., Andeen, G. B., and Kumar, A., 2000, "The Use of an Organic Self-Assembled Monolayer Coating to Promote Drop-

wise Condensation of Steam on Horizontal Tubes," ASME J. Heat Transfer, **122**(2), pp. 278–286.
[13] Vemuri, S., and Kim, K. J., 2006, "An Experimental and Theoretical Study on the Concept of Dropwise Condensation," Int. J. Heat Mass Transfer, **49**(3–4), pp. 649–657.
[14] Vemuri, S., Kim, K. J., Wood, B. D., Govindaraju, S., and Bell, T. W., 2006, "Long Term Testing for Dropwise Condensation Using Self-Assembled Monolayer Coatings of n-Octadecyl Mercaptan," Appl. Therm. Eng., **26**(4), pp. 421–429.
[15] Tanasawa, I., 1991, "Advances in Condensation Heat Transfer," Adv. Heat Transfer, **21**, pp. 55–139.
[16] Fatica, N., and Katz, D. L., 1949, "Dropwise Condensation," Chem. Eng. Prog., **45**(11), pp. 661–674.
[17] Randolph, A. D., 1988, *Theory of Particulate Processes*, 2nd ed., Academic, New York.
[18] Leach, R. N., Stevens, F., Langford, S. C., and Dickinson, J. T., 2006, "Dropwise Condensation: Experiments and Simulations of Nucleation and Growth of Water Drops in a Cooling System," Langmuir, **22**(21), pp. 8864–8872.
[19] Dimitrakopoulos, P., and Higdon, J. J. L., 1999, "On the Gravitational Displacement of Three-Dimensional Fluid Droplets From Inclined Solid Surfaces," J. Fluid Mech., **395**, pp. 181–209.
[20] Kim, H.-Y., Lee, H. J., and Kang, B. H., 2002, "Sliding of Liquid Drops Down and Inclined Solid Surface," J. Colloid Interface Sci., **247**, pp. 372–380.